Quantifying the Efficacy of Weather Forecasting Data for Flight Contrail Optimization

Esther Roosenbrand, Junzi Sun and Jacco Hoekstra
Faculty of Aerospace Engineering, Delft University of Technology
Delft, The Netherlands

***Abstract*—Contrail optimization offers an efficient and cost-effective way for aviation to immediately reduce its climate impact. Open-source optimization, wherein the contrail and emission effects are balanced based on meteorological open data, has been presented in previous work. However, prior research overlooks the importance of using forecasting data, as opposed to post-processed reanalysis data. For contrail optimization to be implementable, forecasting data needs to be available at a sufficient quality in the flight planning stage in order to perform the optimization. In this paper, a fully open non-linear optimal control flight optimization is implemented and applied using both forecasting and reanalysis data. A total of 120 days (175.440 flights) of flight data from OpenSky are used in the analysis. We show that forecasts with larger lookahead times (up to 12 hours) are equally effective when compared to more recent forecasts (1 hour lookahead time) for contrail optimization, with equally high accuracy. However, when compared to more accurate post-processed reanalysis data, there are considerable differences in predicted contrails formed. This research shows there is still a long way to go before we can actually implement contrail optimal flight planning.**

***Keywords*—Sustainability, Contrails, OpenAP, Optimization, OpenSky, Aircraft Surveillance Data**

I. Introduction

Aviation currently accounts for approximately 5% of net anthropogenic climate forcing [1]. This contribution is expected to cause increasingly severe climate impacts as flight numbers rise. Promising measures, such as alternative fuels and aerodynamic aircraft designs, are under development, but their large-scale commercial implementation is expected to take years or even decades. Given the urgency of addressing the climate crisis, sustainable aviation efforts should not only prioritize the advancement of these technologies but also focus on immediate implementations feasible for today's aircraft fleet.

One significant factor contributing to aviation's radiative forcing over shorter timescales is the formation of contrail cirrus, despite some uncertainties regarding the scale of the impact [2]. During the daytime, contrails are understood to have a cooling effect by scattering incoming solar radiation back to space, akin to a parasol. However, both during the day and at night, contrails trap terrestrial radiation, thereby restricting outgoing radiation and causing a warming effect. There is scientific consensus that the net radiative effect of contrails is positive, meaning they contribute to warming the Earth's atmosphere [1]. Contrails have an immediate warming effect, unlike CO_2 emissions, which influence global warming over a span of 20–40 years [3]. This underscores the importance of minimizing contrail formation to mitigate aviation's climate impact, both now and in the future.

Re-routing aircraft to avoid contrail formation generally results in additional fuel burn due to longer flight distances [3]. However, research has shown that significant net environmental savings are possible with minimal operational changes [4], [5]. In [6], we presented a fully 4D non-linear optimal control trajectory optimizer, which considers the wind field and an objective function that considers both carbon emissions and contrail impacts. In [6] the optimizer was used to analyse the environmental savings possible through contrail-minimization for half a million flights based on ECMWF ERA5 Reanalysis data.

Said reanalysis data only becomes available a few hours after actual takeoff. Hence, it is not available for, and cannot be applied in, the flight planning phase. The two methods of contrail optimization are outlined in [7], namely, pre-tactically and tactically. With pre-tactical, a flight is planned more than twelve hours in advance of flight departure, as opposed to tactically, where contrail avoidance is done during the flight (as with the MUAC trail [8]). The efficacy of both methods depends greatly on the accuracy of the predicted contrail formation. Additionally, [7] suggests that aircraft operators could pre-tactically optimize the flight plan's vertical component 12 hours before the flight and finalize the horizontal component of the flight plan with the most up-to-date forecast.

Contrail optimization based on forecasting data is seen in literature [3], [9], [10], [11], [12]. However, these do not include reanalysis data to assess the accuracy of the optimization. Furthermore, in this paper, flights over an entire year are optimized, contributing to understanding the seasonal effects of contrail prediction. Finally, our contrail optimization is unique in its use of solely open-source data and code, in combination with the computational speed and customizability of the objectives.

In this paper, 175.440 flights have been contrail optimized based on pre-tactically available forecasting data, and then the obtained optimization outcome is reviewed using the reanalysis data in order to assess the merit and capabilities of using forecasting data in contrail optimization. This evaluation is an essential step in the field of contrail optimization from the perspective of air traffic management, in order to bring this promising concept closer to implementation.

This paper is structured as follows. Section II explains the background knowledge for the formation of persistent contrails. Section III gives an overview of the collected and used data. Section IV provides the details on the methodologies for this study. Finally, Sections V, VI, and VII include the results, discussions, and conclusion.

II. Contrail formation

Generally, contrails formed at low air temperature conditions, -40 °C (233 K), and at a high relative humidity [13]. In order for a contrail to be persistent and have an environmental impact, two atmospheric conditions must be met:

1) Schmidt-Appleman Criterion (SAC), which states that the temperature must be below the critical temperature.
2) The ambient air is supersaturated with respect to ice ($RH_i > 100\%$) in an ice-supersaturated region (ISSR).

The well-established Schmidt-Appleman criterion [13] is a thermodynamic model that takes into account ambient pressure, humidity, and the water-to-heat ratio in exhaust plumes. As an aircraft flies through atmospheric conditions satisfying SAC, saturation with respect to liquid water occurs, and a contrail is formed.

The specific temperature threshold (T_{LM}) for contrail formation relies on the ambient relative humidity and the slope of the isobaric mixing line (G), which can be defined as follows:

$$G = \frac{EI_{H_2O}\ c_p\ p}{\varepsilon\ Q\ (1-\eta)} \tag{1}$$

where the constants for Eq. (1) can be found in Table I. In this paper, only cruise optimization is applied. A propulsion efficiency of η = 0.3 is assumed for modern aircraft–engine combinations [14].

In order to determine the threshold value T_{LC}, the temperature T_{LM} [13] must first be identified, which is given by:

$$T_{LM} = -46.46 + 9.43\ln(G - 0.053) + 0.72[\ln(G - 0.053)]^2 \tag{2}$$

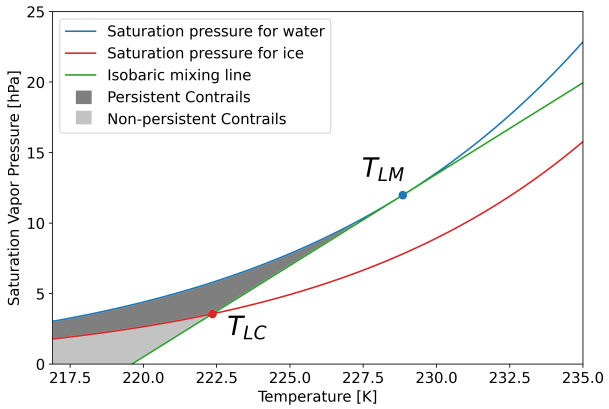

Figure 1. A visualization of the geometric approach to determining the critical formation temperature (T_{LC}), using the saturation pressure for water, the saturation pressure for ice, and the isobaric mixing line with slope G at p_h = 230 hPa. Zones of contrail persistence are also indicated in the graph.

Subsequently, the mixing line is defined as the tangent line at the T_{LM} point with the saturation water vapour pressure curve (e^*). T_{LC} represents the intersection of the mixing line and the saturation water vapour pressure curve over ice. This geometric approach to identifying T_{LC} is visualized in Figure 1. The RH_i (%) can be calculated through the specific humidity (q in %):

$$RH_i = \frac{q\ p\ R_v}{R_d\ e_{ice}} \tag{3}$$

where e_{ice} (hPa) is the actual vapour pressure over ice [15]:

$$\log e_{ice} = 9.550426 - \frac{5723.265}{T} + 3.53068\ln(T) - 0.00728332T \tag{4}$$

where p is pressure, provided by the reanalysis or forecast data. R_v and R_d are gas constants for water vapour and dry air (see Table I).

TABLE I: Constants used for contrail formation

Symbol	Constant	Value	Unit
EI_{H_2O}	Emission index	1.2232	$-\ (kg_{H_2O}\ kg_{fuel}^{-1})$
c_p	Specific heat capacity air	1004	$J\ kg^{-1}\ K^{-1}$
ε	Ratio molar mass of water vapor and air	0.622	-
Q	Specific combustion heat	43×10^6	$J\ kg^{-1}$
η	Overall propulsion efficiency	0.3	-
R_v	Gas constant of water vapour	461.51	$J\ kg^{-1}\ K^{-1}$
R_d	Gas constant of dry air	287.05	$J\ kg^{-1}\ K^{-1}$

III. Data

In total, one full year of ADS-B flight data was gathered and processed for this study, which included 175.440 flights. Both weather forecasts and reanalysis data are also gathered for the experiments. This section explains the data sources and the steps taken before further processing.

A. Flight data

The OpenSky Network has been collecting global air traffic surveillance data since 2013. The unfiltered and raw data from the OpenSky Network, based on ADS-B, Mode S, TCAS, and FLARM messages, are available for use [16]. The variables used in this research include time, latitude, longitude, callsign, and altitude.

In this paper, in order to provide an overview of a year while also effectively using computational capabilities, every three days of data is downloaded, starting from 1st of January 2022 over the European airspace (30 to 70° latitude and -20 to 50° longitude). If there is no contrail formation along a flight trajectory, the flight is not considered in this research. In total 175.440 flights have contrail formation at some point along the trajectory, a total of 33% of all flights.

B. Forecast and Reanalysis data

The ARPEGE (Action de Recherche Petite Echelle Grande Echelle, which translates to research project on small and large scales) is an open global numerical weather prediction model from Météo France, in collaboration with ECMWF. The initial conditions of the forecast are based on the assimilation of a range of conventional observational data (sounding balloons and aircraft, boat buoy and land measurements) and remote sensing data (infra-red and microwave images, temperature and humidity from satellite-GPS signals) [17]. The relative weights between these measurements are estimated using an assimilation of 25 short-range forecast scenarios. These weights and parameterizations have been calibrated over numerous measurement campaigns.

Four times a day forecasts are made, at 00.00, 06.00, 12.00, and 18.00 UTC, with forecasting step time from 0 to 12 hours, at a grid of 0.1° x 0.1° (around 11 km) [17]. The 105 vertical levels range from 10 m above the surface to 70 km. In short, if a forecast is run at 06.00 UTC with a lookahead time of 3 hours, the forecast is valid for 09.00 UTC.

The European Centre for Medium-Range Weather Forecasts (ECMWF) ERA5 Reanalysis dataset provides hourly atmospheric data on a high-resolution grid, which features a horizontal resolution of 0.25 degrees and 37 vertical layers.

The main difference between a reanalysis and a forecast is the amount of 'real' data assimilated into the initial conditions. The reanalysis is obtained by assimilating observations from radiosondes, aircraft, and stations, which is supplemented by satellite observations. These measurements from different sources greatly increase the accuracy of meteorological conditions when compared to the forecasts.

Both ERA5 Reanalysis and ARPEGE are based on 4D-Variational data assimilation, though they differ in their implementation and purpose. While ERA5 maintains a consistent physics package optimized for global, long-term performance, IFS undergoes regular updates with specific regional tuning, particularly for European weather patterns [18].

In both cases, data generated by a weather model is reassessed by assimilating observations, generating a new and improved estimate of the atmospheric state [19]. With reanalysis, observations within a 12-hour time window are incorporated into the assimilation. Reanalysis benefits from the availability of future observations, allowing for an improved historical reconstruction, while IFS focuses on real-time forecasting with a 6-12 hours window and incorporates recent observations.

IV. Methodology

A. Comparing Forecasts and Reanalysis

By its nature, reanalysis data is not available for pre-tactical or tactical planning. However, reanalysis can be used to retroactively determine the amount of contrail formation that occurred during a flight.

Figure 2 illustrates how we couple the flight takeoff time to two forecasts that are used for optimization. The nearest hour to takeoff is represented in the solid and dotted top circles, and the multicolored boxes below indicate the two forecasts to be used for each hour of flights. To create a realistic scenario, the forecast that runs at 00.00, 06.00, 12.00, and 18.00 cannot be used for these hours since these would not be available yet. To mimic the pre-tactical situation, the forecast that runs used the 6 and 12-hour look ahead times are used at 00.00, 06.00, 12.00, and 18.00.

Subsequently, to determine the capabilities of incorporating weather forecast data in flight planning to minimize the environmental impact of contrails, optimizations are run using ARPEGE forecasts and ERA5 Reanalysis atmospheric data. These two forecast-optimized trajectories are then compared with the reanalysis-optimized trajectory through three metrics:

1) Δt: change in flight time,
2) Δd: change in flight distance and
3) $\Delta t_{\text{contrail}}$: change in time of persistent contrail formation.

B. Optimizer

In our previous work [6], a fully open non-linear optimal control flight optimizer for contrail avoidance and emission reduction was presented. A high computational efficiency is achieved by combining the most recent trajectory optimizer, *OpenAP.TOP* [20], and atmospheric data handling tool, *fastmeteo* [21].

In the optimizer, the balance between contrail avoidance and emission reduction is determined through the coefficient of influence (*CoI*), with a high *CoI* emphasizing emission reduction more and low avoiding contrail formation more. Based on the analysis in [6], we concluded that a large number of contrails could be mitigated even with a lower CoI, without significant penalty on additional distance flown, flight time, or CO_2 emissions. For these reasons, a *CoI* of 0.8 was selected for this paper.

C. Data processing

Opensky flights were downloaded for every third day from 2022 and clipped to exclusively contain the start and end of the cruise section and takeoff time. Based on the takeoff time of the flights, the two closest hindsight weather forecasts are downloaded, as explained in section IV-A. The optimizer from [6] is run based on these two forecasts. Finally, this resulting forecast-optimized trajectory is combined with reanalysis data in order to verify the degree of contrail formation along the route during the actual operation. Another optimization is run based on reanalysis data, which is used as a baseline to compare how the pseudo-optimal trajectory using forecast data differs from the real optimal with the best post-op meteorological information.

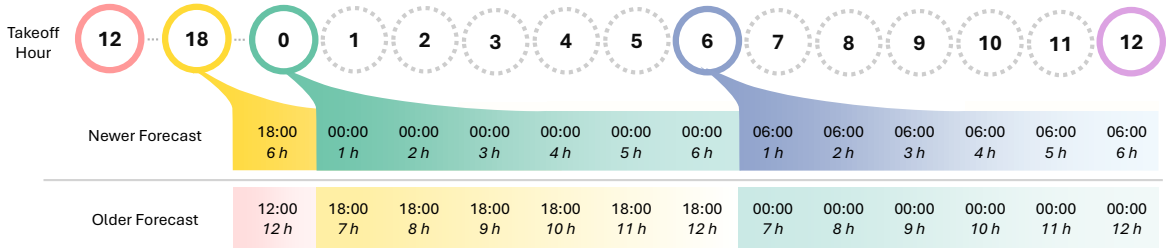

Figure 2. Forecast timeline, where the nearest hour to takeoff is represented in the solid and dotted top circles. The boxes directly below indicate the forecasts used for each takeoff hour. For example, at a 06.00 takeoff time, the newer forecast used is that of 00:00 with a lookahead time of 6 hours, and the older forecast is from 18:00 with a 12-hour lookahead time. This sequence is repeated for hours 12 to 23.

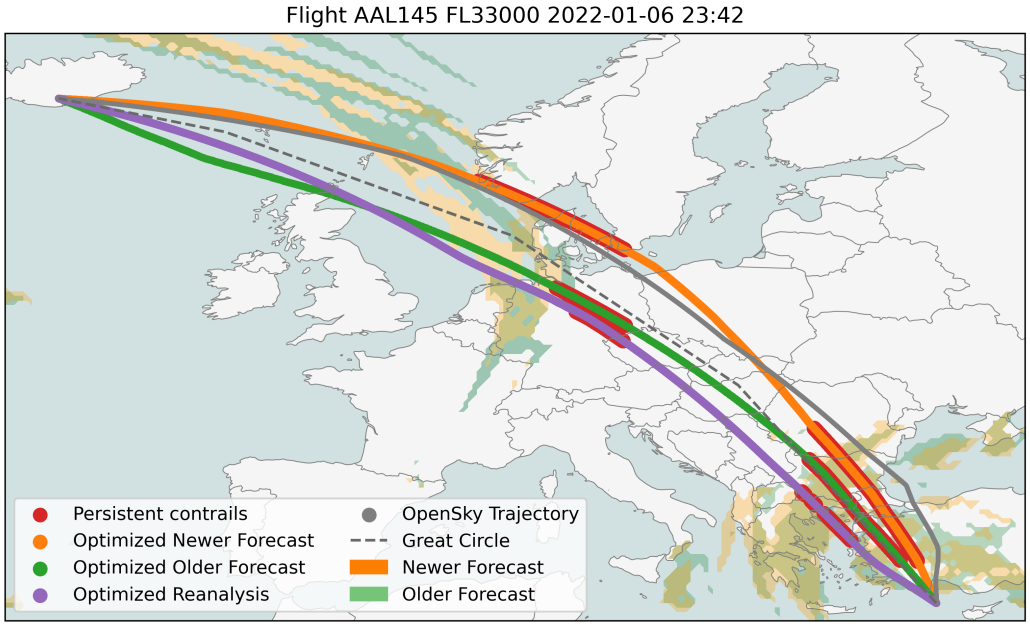

Figure 3. Cruise section of Flight AAL145 from Cyprus to Long Island, New York, United States on the 6th of January 2022. The OpenSky and the three (newer forecast, older forecast and reanalysis) optimized trajectories are shown, together with a grid showing the newer and older forecasts. As only the cruise section within Europe is considered, the flight is cut off over Iceland and starts off the coast of Cyprus.

V. Results

To best illustrate the results and the meaning of the aforementioned metrics, two flights are highlighted in the following sections, after which histograms containing all 175.440 flights are shown.

A. Forecast Optimization

In Figure 3, the two forecasts and the reanalysis optimizations for flight AAL145 from Cyprus to Long Island, New York, United States on the 6th of January 2022, alongside the ADS-B trajectory from OpenSky are shown. The background contours show the newer (orange) and older (green) forecasts used for the optimizations.

The difference between the two forecasts (specifically over the North Sea) causes the two optimizations to differ, where the newer forecast takes a northern route over the great circle, and the older forecast lies more to the south. As can be seen in Table II, the optimization based on the older forecasts has a shorter travel time and distance, as compared to the optimization based on the reanalysis data, while with the newer forecasts, both increase. Besides this, both also have significantly more travel time in persistent contrail forming regions (increases of 61.8 and 43.0% compared to the reanalysis optimization).

TABLE II: Comparison Metrics for Two Forecasts, AAL145

Forecast	Δt [MM:SS]	Δd [km]	$\Delta t_{\text{contrail}}$ [MM:SS]
Newer	+25:20 (+7.0%)	783 (+0.2%)	15:25 (+61.8%)
Older	-19:25 (-5.3%)	39.8 (-0.01%)	7:11 (+43.0%)

In Figure 4, three optimizations for another flight are shown, BCS7JG from Madrid, Spain to Leipzig, also on the 6th of January 2022. In this instance, because the older and newer forecasts align with each other well, the two forecast optimizations produce the same route. This entails that the metrics, when compared to the optimization based on reanalysis data (Table III), the difference is the same for both optimized flights.

TABLE III: Comparison Metrics for Two Forecasts, BCS7JG

Forecast	Δt [MM:SS]	Δd [km]	$\Delta t_{\text{contrail}}$ [MM:SS]
Newer	-02:35 (-2.6%)	40.5 (-3.8%)	6:11 (+55.8%)
Older	-02:35 (-2.6%)	40.5 (-3.8%)	6:11 (+55.8%)

Compared to the two forecasts optimized flights, the reanalysis-optimized flight deviates from the great circle to a greater extent. This causes a comparative decrease in the flight time and distance, as can be seen in Table III. However, the contrail formation along the forecast-optimized routes is significantly more (+55.8%). This is because the reanalysis optimization effectively routes around persistent contrail-forming regions.

B. All Flights

In this section, we provide the aggregated statistics of all 175.440 flights, and the histograms of all these flights are shown for each of the metrics discussed earlier.

1) Changes in flight time: After calculating the total flight time of the three optimized trajectories, based on the older and newer forecasts and the reanalysis, the percent change in flight time was calculated with the reanalysis acting as a baseline.

The histograms in Figure 5 indicate that, on average, the older and newer forecast-based optimizations have shorter flight times (means of -5.4% and -4.7%) compared to the reanalysis-optimized trajectory, due to less ISSR being forecasted in the forecast dataset.

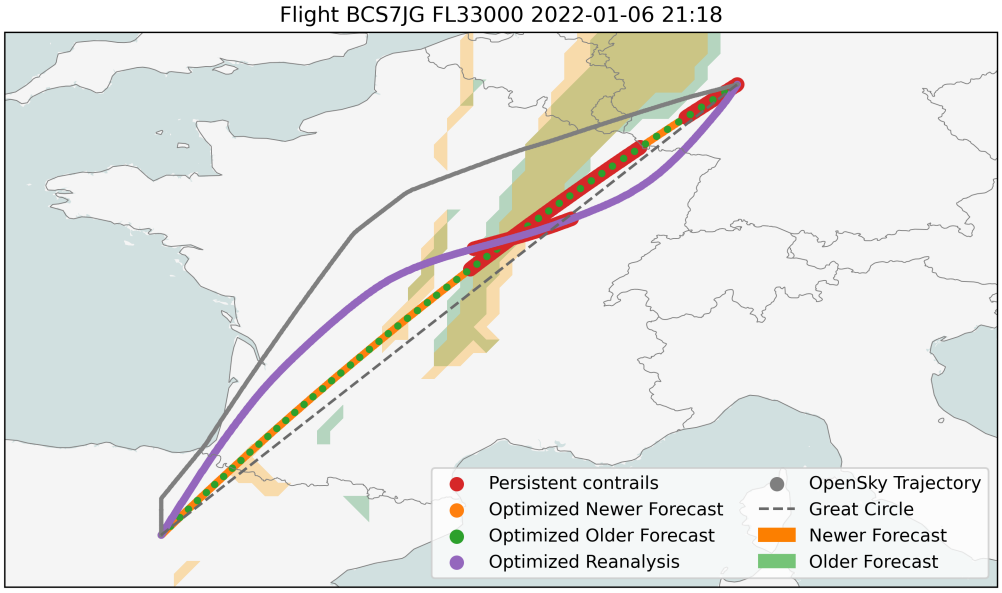

Figure 4. Cruise section of Flight BCS7JG from Madrid, Spain to Leipzig, Germany on the 6th of January 2022. The OpenSky and the three (newer forecast, older forecast and reanalysis) optimized trajectories are shown, together with a grid showing the newer and older forecasts. As only the cruise section is considered, the flight is cut off before reaching Madrid and Leipzig.

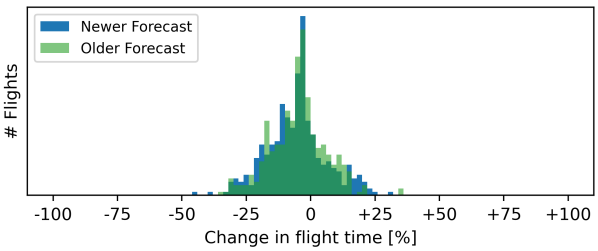

Figure 5. Histogram of the change in flight time for newer (blue) and older (green) forecast- vs reanalysis- optimized trajectories.

2) Changes in flight distance: Figure 6 shows a histogram indicating the change in the flown distance. Both distributions of the two forecast vs. reanalysis contrail optimized trajectories exhibit a normal distribution centered around -2.1 (older) and -1.4 (newer), indicating a slight increase in flight distance for the forecast optimizations. This is related to the previous observation on flight time.

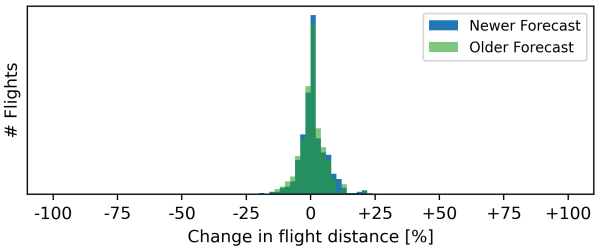

Figure 6. Histogram of the change in flight distance for newer (blue) and older (green) forecast- vs reanalysis- optimized trajectories.

3) Changes in time of persistent contrails: The third histogram of Figure 7 shows the change in time flown in persistent contrail forming conditions (or *contrail time*). The histograms in Figure 7 indicate a large spread from no change to a maximum of 88% increase of contrail time in the forecast-optimal trajectories when compared to reanalysis-optimal trajectories.

Since only flights that form persistent contrails along some section of the trajectory are optimized, there are no cases of a change relative to 0 minutes of contrail time. There are also no cases where the forecast had a shorter travel time than the reanalysis-optimized trajectories, which makes physical sense. On average, the median/mean increase in contrail time when using the newer and older forecasts are very similar, which are 28.9/29.9 and 24.9/24.8, respectively.

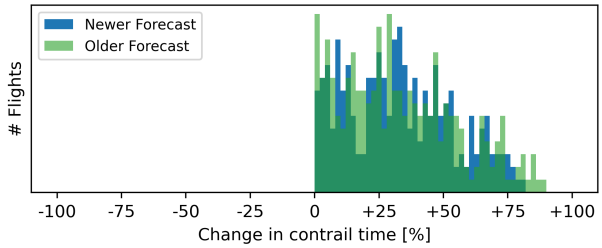

Figure 7. Histogram of the change in contrail time for newer (blue) and older (green) forecast- vs reanalysis- optimized trajectories.

C. Precision, Recall and Accuracy of Forecast

Figure 8 shows a comparison between two forecasts and their persistent contrail forming regions, and of the reanalysis data for the same time and location. Figures 8.a and b show two forecasts with different lookahead times, and Figure 8.c shows the reanalysis data set.

Even though the forecasts are run 6 hours apart, *and* with a long lookahead time of 9 hours, we see alignment in the forecast locations of persistent contrail formation. When comparing these two forecasts with the reanalysis, we see that generally that the location of the regions with persistent contrail formation predicted by the forecasts and the reanalysis weather

forecast correlate to a high extent, but the extent of the regions is underestimated in the forecast. In this section, using three metrics of precision, recall and accuracy, the performance of the forecast is evaluated against the reanalysis.

These three metrics are commonly applied to binary classification tasks, based on the principle of True Positives (*TP*), False Positives (*FP*), True Negatives (*TN*), False Negatives (*FN*).

- Precision is the ratio of correctly predicted positive observations to the total predicted positive observations, or *TP* / (*TP* + *FP*).
- Recall is the ratio of correctly predicted positive observations to all the observations, or *TP* / (*TP* + *FN*).
- Accuracy measures the proportion of correctly classified observations from the total number of observations, or (*TP* + *TN*) / (*TP* + *TN* + *FP* + *FN*).

Table IV shows the values of these three error metrics for the two forecasts as well as for the two contrail forming conditions, SAC and ISSR (see Section II), and the combination of the two for persistence.

TABLE IV: Error Metrics for Both Forecasts

	Precision	Recall	Accuracy
SAC Forecast 1	0.476	0.477	0.353
SAC Forecast 2	0.476	0.476	0.353
ISSR Forecast 1	0.231	0.225	0.885
ISSR Forecast 2	0.223	0.223	0.886
Persistent Forecast 1	0.269	0.295	0.929
Persistent Forecast 2	0.261	0.291	0.929

The three error metrics were determined for the hourly forecasts over the entire year. In Figure 9, the error metrics are shown as a weekly average. Older forecasts are shown as dotted lines in contrasting colors to the newer forecast's solid lines. Figure 9 shows the three error metrics are essentially the same, with the maximum difference being 0.01 for precision and recall and 0.001 for accuracy. An increase in precision and recall during the colder winter months for the Schmidt-Appleman criterion (SAC) is also observed. Most likely, this is due to there being more SAC-satisfying atmospheric conditions [22] in the colder winter months, and so the precision and recall will be higher.

As this forecast and reanalysis comparison is computed hourly for two lookahead times, we can also investigate a change in metrics caused by these varying lookahead times. This is visualized in Figure 10. Similarly, no significant change is observed here with increasing lookahead time for all three of the persistent contrail forming conditions.

VI. Discussion

A. Forecasts and Reanalysis comparison

Based on the accuracy, precision, and recall metrics shown in Section V-C, we see that the forecasts underestimate the regions where persistent contrails form, specifically for the ISSR criterion. The extra contrail time in forecast-optimized trajectories compared to reanalysis optimized is around 25%, which shows a significant issue of using forecast data to perform pre-tactical contrail minimization. The shorter flight time and flight distance seen in Figures 5 and 4 indicate this as well, where because less persistent contrails regions are predicted, fewer deviations are necessary, and the flight can prioritize fuel optimization to a greater extent.

This aligns with what is seen in [23], where a comparison is made between an IFS (similar to the ARPEGE data used here) and WRF forecasts. It states that WRF (Weather Research and Forecasting) models, which incorporate multi-moment cloud physics, offer a higher accuracy in the relative humidity with respect to ice than IFS (Integrated Forecast system) models.

The analysis could be extended to include various other forecasts, such as the WRF model, but also NOAA's GFS or the HRRR, which is already applied in aviation planning, in wind-optimization, severe weather avoidance and turbulence. While both the suggested forecasts and reanalysis are publicly available, it is at lower vertical and temporal resolution.

B. Forecasts comparison

Figures 9 and 10 show that the newer and older forecasts align to a great extent, with very small differences, between the two. This is confirmed by the histograms in Figures 5, 6, and 7, where the two histograms in green and blue overlap as well. This indicates that the older forecasts are just as effective at predicting conditions for persistent contrail formation as those made closer to the actual flight time.

C. Cooling effect of the contrails

As described in the Introduction, contrails can have both warming and cooling effects on the climate, although the net radiative effect of contrails is positive and so warming.

Currently, the cost function presented in this paper is constructed as a Coefficient of Impact (CoI) between avoiding persistent contrail forming regions and fuel. This means that forming potentially cooling contrails is also avoided. In future work, based on meteorological and geographical data, a prediction can be made whether the persistent contrail formed will be warming or cooling can be made. Besides this incorporation, instead of a CoI between contrails and fuel, a radiative forcing-based ratio could be used.

D. Safety of diverted flight trajectories

In this paper, each trajectory is optimized individually, and the complete air network is not taken into account. This implies that it is possible for two flights post-optimization to no longer be horizontally or vertically separated. However, safety impacts are minimal [24], with only a slight increase in the number of intrusions or conflicts when changing altitudes for contrail prevention.

E. Uncertainty ERA-5 weather data

The presence of persistent contrails is determined using ECMWF's ERA5 dataset through the temperature and specific humidity parameters. The temperature condition mentioned in Section II can be predicted reliably [25].

However, the specific humidity parameter has some problems with reliability, especially in the upper troposphere. The level of relative humidity over ice is often underestimated [26].

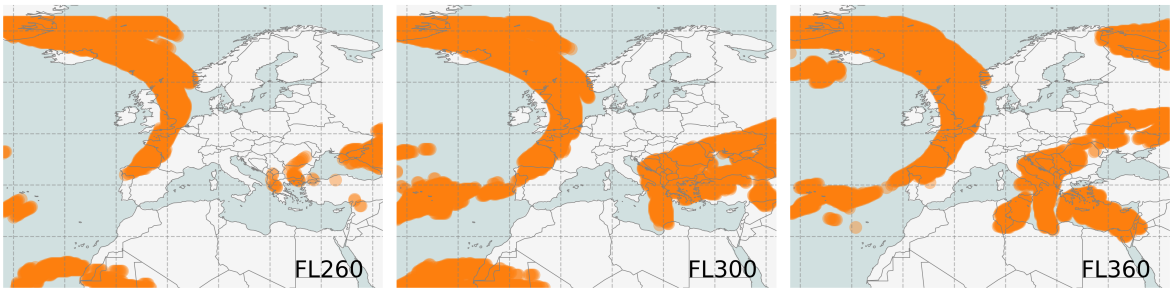

(a) ARPEGE forecast from the 6th of January 2022 at 12:00 UTC, with a lookahead time of 3 hours.

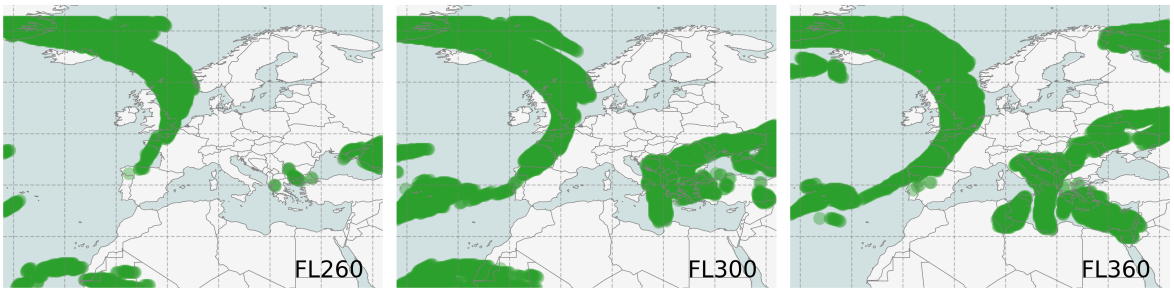

(b) ARPEGE forecast from the 6th of January 2022 at 06:00 UTC, with a lookahead time of 9 hours.

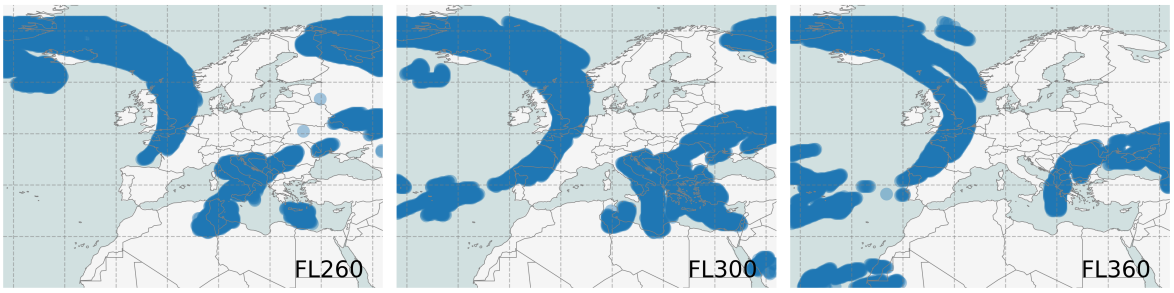

(c) ECMWF Reanalysis ERA-5 of the 6th of January 2022, 15:00 UTC.

Figure 8. Illustration of two persistent contrail forecasts (a and b) and reanalysis (c) of the same time and location for several flight levels.

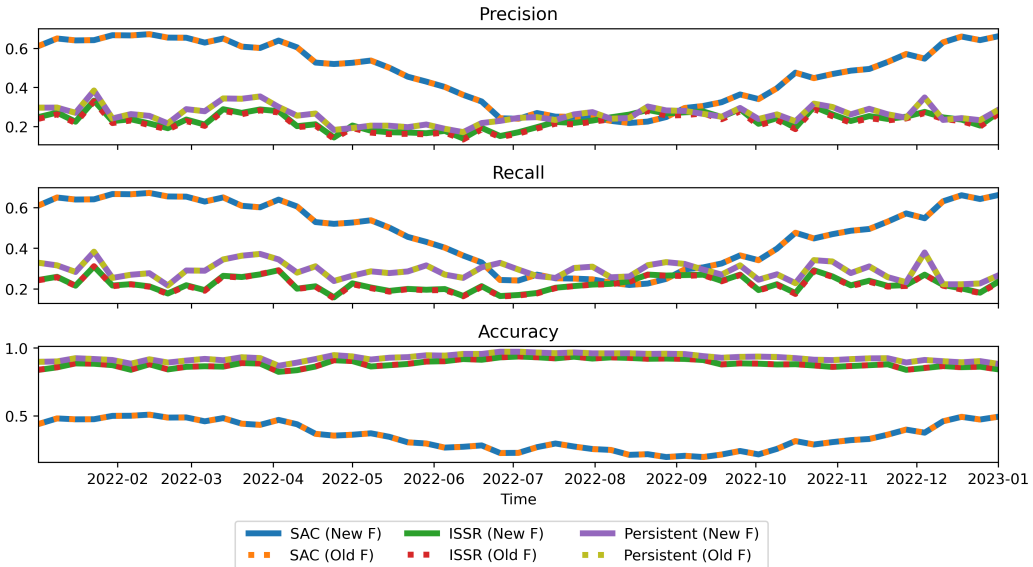

Figure 9. Weekly averages of the three error metrics; precision, recall and accuracy for the two persistent contrail forming condition (SAC and ISSR) and the combination of these two. These metrics are presented for the new (solid lines) and old (dotted lines) forecasts. The two forecasts are essentially equal, with a maximum difference between the two being 0.01 for precision and recall and 0.001 accuracy.

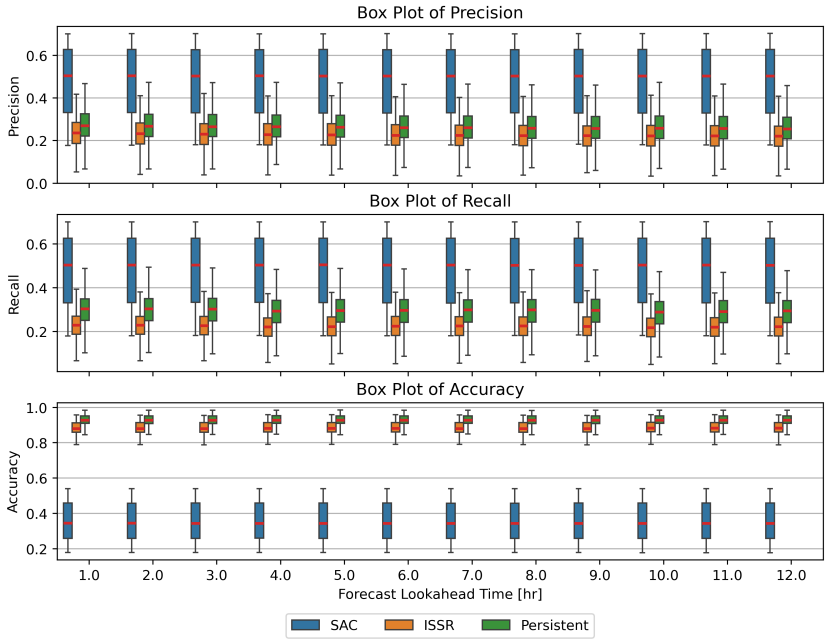

Figure 10. Box plots of the three error metrics: precision, recall, and accuracy for the lookahead times of the forecasts. The metrics do not change significantly with increasing forecast lookahead times.

This leads to an underestimation of the instantaneous radiative forcing [25]. Before strategies of contrail optimization, like the ones presented in [7], become operational, the prediction of ice supersaturation needs to be more reliable.

F. Improvements Schmidt-Appleman Criterion

In this paper, a propulsion efficiency of $\eta = 0.3$ is assumed for modern aircraft–engine combinations. However, in Eq. (1) η is defined as the fraction between resulting energy (thrust and true airspeed) and required energy (specific combustion heat Q and fuel flow) [13]. In future work, this parameter should be dynamic and not assumed constant.

VII. Conclusion

This paper investigates the capabilities of using forecast data in contrail optimization. From an air traffic management perspective, this is an essential step in integrating contrail optimization into the flight planning process, as opposed to using post-reanalysis atmospheric data. To analyse the merits of forecasting data, a year of OpenSky flight data from 2022, 175.440 flights, was gathered and optimized.

Two ARPEGE forecasts with different run times were used in the optimization, an older and a new one. Despite the older forecast having a lookahead time ranging from 12 to 7 hours, from our analysis, we conclude that the older forecasts are just as effective at predicting persistent contrail forming conditions as the use of forecasts closer to the actual takeoff time of the flight. While the error analysis shows that overall precision and recall are lacking in comparison to more reliable reanalysis data, the accuracy of the persistent contrail forming conditions, upon which optimization is run, is high.

Both these conclusions, based on analysis from two weather products, indicate that incorporating contrail optimization into flight planning at an early stage in the process is possible, with ample time before takeoff. However, due to the inaccuracies in contrail-forming meteorological conditions in weather forecast data, there is a large increase of actual contrail time when compared with reanalysis-optimal trajectories. This hinders the effectiveness of pre-tactical flight contrail-minimization.

References

[1] D. Lee, "The contribution of global aviation to anthropogenic climate forcing for 2000 to 2018.," *Atmospheric Environment*, vol. 244, 2021.

[2] V. Grewe, K. Dahlmann, J. Flink, C. Frömming, R. Ghosh, K. Gierens, R. Heller, J. Hendricks, P. Jöckel, S. Kaufmann, *et al.*, "Mitigating the climate impact from aviation: Achievements and results of the dlr wecare project," *Aerospace*, vol. 4, no. 3, p. 34, 2017.

[3] D. Avila, L. Sherry, and T. Thompson, "Reducing global warming by airline contrail avoidance: A case study of annual benefits for the contiguous united states.," *Transportation Research Interdisciplinary Perspectives*, vol. 2, 2019.

[4] B. Sridhar, H. Ng, F. Linke, and N. Chen, "Benefits analysis of wind-optimal operations for transatlantic flights," *14th AIAA Aviation Technology, Integration, and Operations Conference*, 2014.

[5] J. Rosenow and H. Fricke, "Luchkova et al. minimizing contrail formation by rerouting around dynamic ice-supersaturated regions," *Aeron Aero Open Access J*, vol. 2, no. 3, pp. 105–111, 2018.

[6] E. Roosenbrand, J. Sun, and J. Hoekstra, "Flight optimization for contrails and emissions: A large-scale trade-off analysis using open data and models," in *Proceedings of the 11th International Conference for Research in Air Transportation*, July 2024.

[7] J. Molloy, R. Teoh, S. Harty, G. Koudis, U. Schumann, I. Poll, and M. E. Stettler, "Design principles for a contrail-minimizing trial in the north atlantic," *Aerospace*, vol. 9, no. 7, p. 375, 2022.

[8] R. Sausen, S. M. Hofer, K. M. Gierens, L. Bugliaro Goggia, R. Ehrmantraut, I. Sitova, K. Walczak, A. Burridge-Diesing, M. Bowman, and N. Miller, "Can we successfully avoid persistent contrails by small altitude adjustments of flights in the real world?," *Meteorologische Zeitschrift*, 2023.

[9] A. M. Frias, M. Shapiro, Z. Engberg, R. Zopp, M. Soler, and M. E. J. Stettler, "Feasibility of contrail avoidance in a commercial flight planning system: an operational analysis," *Environmental Research: Infrastructure and Sustainability*, vol. 4, no. 1, p. 015013, 2024.

[10] J. Rosenow and H. Fricke, "Individual condensation trails in aircraft trajectory optimization," *Sustainability*, vol. 11, no. 21, p. 6082, 2019.

[11] B. Sridhar, H. Ng, and N. Chen, "Integration of linear dynamic emission and climate models with air traffic simulations," *AIAA Guidance, Navigation, and Control Conference*, p. 4756, 2012.
[12] B. Sridhar, N. Y. Chen, H. K. Ng, and F. Linke, "Design of aircraft trajectories based on trade-offs between emission sources," *9th USA/Europe Air Traffic Management Research and Development Seminar*, 2011.
[13] U. Schumann, "Formation, properties and climatic effects of contrails," *Comptes Rendus Physique*, vol. 6, no. 4-5, pp. 549–565, 2005.
[14] A. Rap, P. Forster, A. Jones, O. Boucher, J. Haywood, N. Bellouin, and R. De Leon, "Parameterization of contrails in the uk met office climate model," *Journal of Geophysical Research: Atmospheres*, vol. 115, no. D10, 2010.
[15] D. M. Murphy and T. Koop, "Review of the vapour pressures of ice and supercooled water for atmospheric applications," *Quarterly Journal of the Royal Meteorological Society: A journal of the atmospheric sciences, applied meteorology and physical oceanography*, vol. 131, no. 608, pp. 1539–1565, 2005.
[16] M. Strohmeier, X. Olive, J. Lübbe, M. Schäfer, and V. Lenders, "Crowdsourced air traffic data from the opensky network," *Earth System Science Data*, vol. 13, no. 2, pp. 357–366, 2021.
[17] W. France, "The arpège and arome digital weather forecasting systems from météo-france," *Paris, France, 8p*, 2015.
[18] M. Déqué, C. Dreveton, A. Braun, and D. Cariolle, "The arpege/ifs atmosphere model: a contribution to the french community climate modelling," *Climate Dynamics*, vol. 10, pp. 249–266, 1994.
[19] H. Hersbach, B. Bell, P. Berrisford, S. Hirahara, A. Horányi, J. Muñoz-Sabater, J. Nicolas, C. Peubey, R. Radu, D. Schepers, *et al.*, "The era5 global reanalysis," *Quarterly Journal of the Royal Meteorological Society*, vol. 146, no. 730, pp. 1999–2049, 2020.
[20] J. Sun, "Openap.top: Open flight trajectory optimization for air transport and sustainability research," *Aerospace*, vol. 9, no. 7, p. 383, 2022.
[21] J. Sun and E. Roosenbrand, "Fast contrail estimation with opensky data," *Journal of Open Aviation Science*, vol. 1, no. 2, 2023.
[22] E. Roosenbrand, J. Sun, and J. Hoekstra, "Examining contrail formation models with open flight and remote sensing data.," *SIDS 2022*, 12 2022.
[23] G. Thompson, C. Scholzen, S. O'Donoghue, M. Haughton, R. L. Jones, A. Durant, and C. Farrington, "On the fidelity of high-resolution numerical weather forecasts of contrail-favorable conditions," *Available at SSRN 4844490*, 2024.
[24] E. Roosenbrand, J. Sun, and J. Hoekstra, "Contrail minimization through altitude diversions: A feasibility study leveraging global data," *Transportation Research Interdisciplinary Perspectives*, vol. 22, p. 100953, 2023.
[25] K. Gierens, S. Matthes, and S. Rohs, "How well can persistent contrails be predicted?," *Aerospace*, vol. 7, no. 12, 2020.
[26] S. M. Hofer, K. M. Gierens, and S. Rohs, "How well can persistent contrails be predicted? – an update," *EGUsphere*, vol. 2024, pp. 1–24, 2024.